Journal of Applied Sciences

ISSN 1812-5654

science alert

ANSInet
an open access publisher
http://ansinet.com

Journal of Applied Sciences 15 (3): 483-491, 2015
ISSN 1812-5654

ansinet
Asian Network for Scientific Information

RESEARCH ARTICLE OPEN ACCESS

DOI: 10.3923/jas.2015.483.491

Intensity Modulated Radiation Therapy Plans Verification Using a Gaussian Convolution Kernel to Correct the Single Chamber Response Function of the I'mRT MatriXX Array

S. Alashrah and A. El-Taher
Department of Physics, College of Science, Qassim University, Qassim, Saudi Arabia

ARTICLE INFO
Article History:
Received: November 08, 2014
Accepted: January 01, 2015

Corresponding Author:
A. El-Taher,
Department of Physics,
College of Science, Qassim University,
Qassim, Saudi Arabia

ABSTRACT
Low spatial resolution in the penumbra region is normally encountered in a 2D array I'mRT MatriXX which is commonly used in verifying Intensity Modulated Radiation Therapy (IMRT) plans. Low spatial resolution results from the size of a detector and the transport of secondary electrons from the walls into the measuring volume. In this study, a Gaussian convolution kernel was chosen to convolve the true dose profile of five nasopharynx IMRT plans calculated by Treatment Planning System (TPS). Gafchromic film (EBT2) and Monte Carlo simulation were also used to verify the true dose profile. The head of a LINAC (Artiste) and dose distribution in a water phantom for the selected field sizes were simulated using the EGSnrc (BEAMnrc/DOSXYZnrc) code and then compared to the ion chamber measurements. Good agreement in the dose profiles between I'mRT MatriXX, IC03, EBT2 film and the Monte Carlo simulation were observed in the low gradient region. In the steeper dose gradients better agreement between I'mRT MatriXX and IC03 was obtained after the Gaussian convolution kernel was applied to the IC03 data. The convolved dose distribution for IMRT plans were compared with the measured plans of a 2D array I'mRT MatriXX. The passing rates improved significantly from 80.2-92.2% using the 3%/3 mm gamma index criteria when compared to cross dose profile plans from the treatment planning system after convolution correction. Convolution can minimize the difference in the beam profiles which occur due to the limited resolution of the I'mRT MatriXX detector.

Key words: Gaussian convolution kernel, I'mRT MatriXX, IMRT plan verification, radiation therapy

INTRODUCTION

Several techniques in beam delivery have been developed to have precise conformed dose profiles. One such technique is Intensity-Modulated Radiation Therapy (IMRT) where improved dose conformity to target and a reduced dose to the surrounding healthy tissues is the goal. The IMRT uses non-uniform radiation beam intensities as well as small segments which are determined using computer based optimization techniques. The dose distribution on the target can be further shaped by modulating the intensity of each field used. Normally IMRT has steep dose gradients which would require the use of infinitely small detectors. This would ensure that the electron fluence across the detector is uniform and no correction has to be made for the volume averaging effect of the detector. Then it is possible to match the calculated Treatment Planning System (TPS) with the dose delivered to the patient. However this is not possible with I'mRT MatriXX which has finite size detectors.

In the final step of the Quality Assurance (QA) of patient specific IMRT plan is to ensure close matching between the dose delivered to the patient and the dose calculated by the TPS. For the dosimetric plan verification, the treatment plan is recalculated in a QA phantom with all the beams perpendicular to the phantom surface. The planar dose distribution is then commonly verified using either films or 2D array pixel ionization chambers. Radiographic films are widely used as they have good spatial resolution but they have to be calibrated against dose.

Gafchromic films which have been refined for clinical radiotherapy dosimetry (Chu *et al*., 1990; Devic *et al*., 2004) are self developing and require no physical/chemical processing. The EBT2 film has low energy dependence, high spatial resolution, insensitive to normal room light (Arjomandy *et al*., 2008; Arnfield *et al*., 2005; Richley *et al*., 2010; Vandana *et al*., 2011). However these films are normally scanned after a 24 h post-irradiation and the results are not immediately available (Kamomae *et al*., 2011; Zeidan *et al*., 2006). The 2D array pixel ionization chambers provides direct measurement of dose without frequent calibration and the measurements are in real time (Alashrah *et al*., 2010; Herzen *et al*., 2007; Spezi *et al*., 2005).

The poor resolution of the 2D array pixel ionization chambers in the steeper dose gradients which occur in the penumbra regions has been attributed to the finite size of the single detector in the 2D array as well as the transport of secondary electrons from the walls into the measuring volume (Li *et al*., 2009; Poppe *et al*., 2007). This disadvantage can be overcome by the method proposed by Poppe *et al*. (2006) who convolved the true dose profile provided by the TPS with the response function of the single ionization chamber and used the convolution product for the gamma-index based comparison with the measured 2D array profile.

The single detector's dose response function of the I'mRT MatriXX array can be defined as the convolution kernel k(x) that transforms the true dose profile R(x) into the measured signal profile D(x) and thereby characterizes the broadening of the slit-beam dose profile (Charland *et al*., 1998; GagoArias *et al*., 2012; Looe *et al*., 2013; Van't Veld *et al*., 2001). It is affected by the detector size, the replacement of water by air, the wall and the central electrode of the detector as well as the geometrical form of the chamber itself (Looe *et al*., 2013; Van't Veld *et al*., 2001). As the ranges of high-energy secondary electrons traversing each chamber are relatively large, the measured chamber signal is not only due to secondary electrons entering the chamber from the front side but also from the ridges between the single chambers (Alashrah *et al*., 2013). Therefore, each ion chamber has a dose response function which is also affected by the transport of secondary electrons.

The dose response functions for I'mRT MatriXX detector were obtained at a shallow depth of 0.5 cm and at a depth of 5 cm which is beyond the depth dose maximum (d_{max}) for a nominal photon energy of 6 MV (Alashrah *et al*., 2013). At the depth beyond the dose maximum, the dose response function of the I'mRT MatriXX can be characterized by a Gaussian function (Alashrah *et al*., 2013). Similar results were obtained by several authors (Bednarz *et al*., 2002; Fox *et al*., 2010; Gago-Arias *et al*., 2012; Garcia-Vicente *et al*., 2000; Looe *et al*., 2013; Pappas *et al*., 2006; Ulmer and Kaissl, 2003; Yan *et al*., 2008). They concluded that the Gaussian convolution kernels are the best fit function to describe the detector response function beyond d_{max}. Looe *et al*. (2013) have recently recognized that the Gaussian shape is in reality a good approximation to the more detailed true shape of the convolution kernel, providing the same low-pass filtering of the spatial frequency spectrum. Fox *et al*. (2010) found that the shaping parameter of the Gaussian convolution kernel was dependent on the depth measurement. However, Yan *et al*. (2008) found that the detector response function was independent of both field size and depth beyond the depth dose maximum.

The deconvolution method can also be applied to solve the poor resolution of the I'mRT MatriXX. The measured values of the array chambers are deconvolved with the response function of a single chamber. The expected values are compared with the planned values. However, this is not possible in practice, as the measured values are only known at the grid width of the chamber centers (Poppe *et al*., 2006). Furthermore, dividing by the kernel at high frequencies involves dividing by very small numbers which is equivalent to multiplication by very large numbers and this will strongly affect the deconvolution result (Bednarz *et al*., 2002).

The basic dosimetric properties of a commercialized array of 2D pixel ionization chambers I'mRT MatriXX used in this study was reported in a previous study of Alashrah *et al*. (2010). These tests included the location of the effective point of measurement, dose linearity, energy dependence, the start-up behavior of the I'mRT MatriXX, field size dependence, dose rate effect and the stability of the detector over time. The depth dependence of the single chamber response function of the I'mRT MatriXX array in a 6 MV photon beam was studied in a previous paper (Alashrah *et al*., 2013). Here at a depth beyond the dose maximum, the dose response function of the I'mRT MatriXX can be characterized by a Gaussian function (Alashrah *et al*., 2013).

In this study, a true beam profile obtained by Treatment Planning System (TPS) was convolved with Gaussian convolution kernel to fit the response function of a finite size of a single detector in the I'mRT MatriXX 2D array for five nasopharynx IMRT plans. All measurements were performed at beyond the depth dose maximum (d_{max}). Gafchromic (EBT2) film and EGSnrc (BEAMnrc/DOSXYZnrc) were also used in this study as a high spatial resolutions are obtained especially in the steeper dose gradient regions.

MATERIALS AND METHODS

2D array I'mRT MatriXX: A pixel-segmented ionization chamber, I'mRT MatriXX, (Scanditronix Wellhöfer, Germany), was designed to ease the 2-dimensional verification of fields with complex shapes like IMRT. The detector features a 32×32 matrix into 24×24 cm^2 active area divided in 1020 independent vented parallel plate ion chambers. There are no ion chambers at the four corners (Han *et al*., 2010). The sensitive volume of each signal ionization chamber is 0.08 cm^3 (4.5 mm diameter×5 mm height). The ionization chambers are equally spaced with a center to center distance of 0.76 cm. The minimum sampling acquisition time is 20 msec. The buildup material in the detector is made from acrylonitrile butadiene styrene. It is 3.3 mm thick and its density is 1.06 g cm^{-3} as

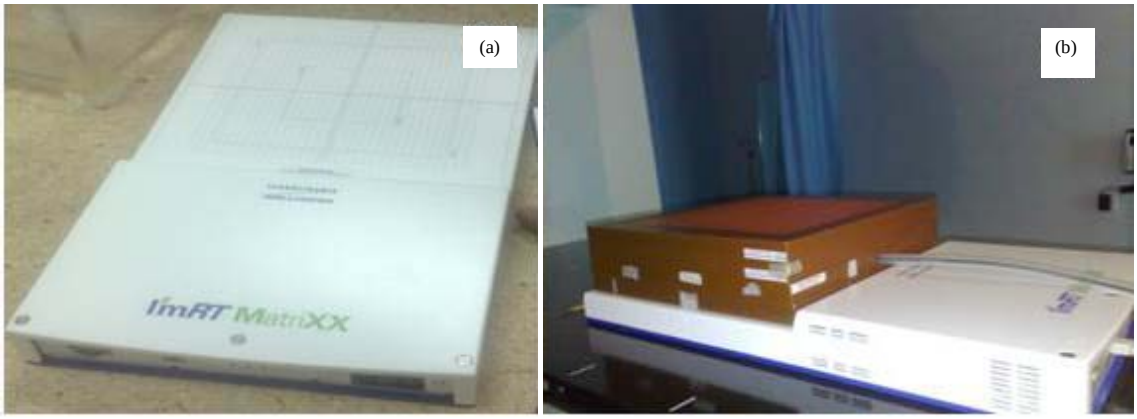

Fig. 1(a-b): (a) 2D array I'mRT MatriXX and (b) Setup of the I'mRT MatriXX used for patient specific IMRT QA comparison with TPS

shown in Fig. 1. The software used for communication and data acquisition with the I'mRT MatriXX is OmniPro-I'mRT software (Scanditronix Wellhöfer, Germany). The calibration and the uniformity correction of I'mRT MatriXX detector was done by the manufacturer. This calibration was verified by comparing I'mRT MatriXX results with a Farmer ionization chamber (FC65-G) at a depth of 5 cm depth in the RW3 solid water phantom and the variation was less than 0.5%. The background radiation was subtracted from the readings. The detector was exposed to levels above 1500 cGy and required an initial warm-up of 60 min for the detector readings to be stable (Alashrah *et al*., 2010). The effective depth of the detector was taken from the manufacturer-specified value of 3.6±0.1 mm. For alignment purpose, there are three marks on the three sides of the detector.

All measurements were performed with x-rays from a Siemens Artiste accelerator (6 MV) in a solid water phantom (RW3). The radiation beam was perpendicular to the phantom surface and the 2D array for all measurements. Beam profile measurements of the five IMRT plans were obtained using 8 cm of solid water phantom on the surface the I'mRT MatriXX 2D array and the distance from source to the effective point of measurement (EFOM) was 100 cm. For all IMRT plans, the measurements were performed using 6 MV photons.

Convolution correction method: Beam broadening in the penumbra region is encountered in a 2D array I'mRT MatriXX especially for small field sizes. This results from the detector size and the transport of secondary electrons from the walls into the measuring volume. This is mathematically modeled by the convolution of the true beam profile with a convolution kernel representing the response function of the single detector. A convolution kernel was chosen to convolve the true dose p rofile to closely fit the dose profile from 2D array I'mRT MatriXX for selected small fields:

$$D_m(x) = \int_{-\infty}^{+\infty} R(u).k(x-u)\,du \qquad (1)$$

where, $D_m(x)$ is the measured dose profile and is described as the convolution of the true beam profile R(u) with the single detector's dose response function k(x-u) (Bednarz *et al*., 2002). MATLAB R2009a was then used to convolve the true dose profile with the Gaussian function at each IC03 reading. This would reduce the deviation from the measured profiles at both the steep and low gradient regions.

Ionization chamber (IC03) for true beam profile: For all the true beam profiles, a small graphite thimble chamber 0.028 cm^3 Wellhöfer chamber (IC03) was used to provide high spatial resolution measurements in the penumbra regions as it had no energy and field size dependence (Lydon, 2005; Meeks *et al*., 1999). This chamber is sufficiently small (0.028 cm^3 active volume). Its length and diameter is 3 mm. Hence, the volume effects like the lack of lateral electronic equilibrium of narrow beams are minimized especially at the steep dose gradients (Fischer *et al*., 2010). Furthermore, it satisfies the recommendation of Paskalev *et al*. (2002) that the detector is 6-7 times smaller than the nominal field size (Lydon, 2005). The measurements using IC03 were performed in a water phantom. In commissioning the linear accelerator for clinical use, all collected data was from IC03 which was then used in the treatment planning system.

Gafchromic film (EBT2): A single box of 25 sheets of Gafchromic EBT2 film (lot No. A052810-02BA) was used in this investigation. Film pieces (5×3 cm^2) were irradiated with 6 MV photons at 5 cm depth in the solid water phantom. The field size used was 10×10 cm^2 at SSD of 100 cm. EBT2 film sheets were used for beam profile measurements (2×2, 5×5, 8×8, 10×10, 15×15 cm^2) using the similar setup used for calibration but using100MUs.

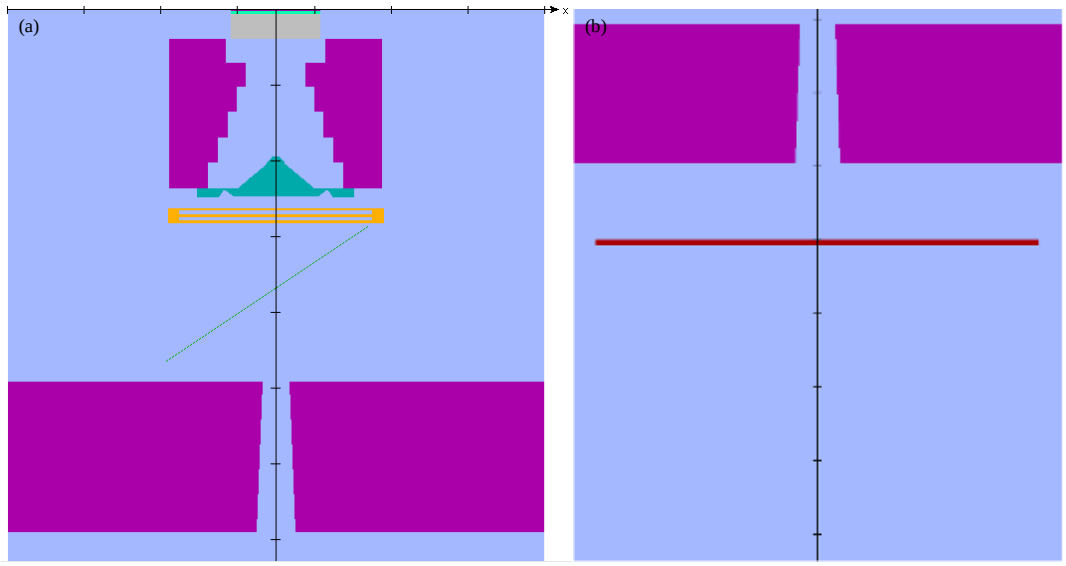

Fig. 2(a-b): Schematic diagram of siemens artiste accelerator (6 MV). The parts including the radiation source, target, the primary collimator, fitting filter, ion chamber, mirror and secondary collimators were simulated according to the manufacture's data, (a) Geometry of the linac head in x-z axis and (b) Geometry of the linac head in y-z axis

The films were scanned two days after irradiation in the portrait mode using the EPSON (EPSON perfection V700 photo) scanner. The exposed films were scanned ten times using the transmission-mode at 48 bit color (red, green, blue) and at a resolution of 72 dpi (Richley *et al*., 2010). The Image J (http://rsb.info.nih.gov) program was then used to extract the red component of the Red-Green-Blue (RGB) range (Matney *et al*., 2010). Subsequently, the net Optical Densities (ODs) of the irradiated films were determined. The net ODs were converted to dose by using the calibration curve and normalized to the maximum dose to obtain the beam profiles of the different field sizes. The results were then compared with those obtained using the ionization chamber (IC03). The film was a second method selected to obtain the true dose profiles for different field sizes.

Monte Carlo Simulation EGSnrc (BEAMnrc/ DOSXYZnrc): The EGSnrc (BEAMnrc/DOSXYZnrc) code (Chetty *et al*., 2007; Rogers *et al*., 1995, 2006) was used to simulate photon beam in this study to generate a true beam profile under the same setup as the scanning measurements. Siemens Artiste accelerator (6 MV) was modeled using the BEAMnrc according to the manufacture's data on the treatment head geometry. Figure 2 shows the 2-dimensional geometrical layout of the component modules of the head LINAC which were SLABS, FLATFILTR, CHAMBER, MIRROR, JAWS and SLABS which determine the phase space occupation at 100 cm from the source. The effect of leakage of MLC was investigated by Tacke *et al*. (2008) and it was low (0.37%). The phase space file contains the position, energy, charge and weight of scored particles in this plan (Alashrah *et al*., 2014). For the BEAMnrc program, ECUT was 0.7 MeV (total energy), PCUT was 0.01 MeV and Directional Bremsstrahlung Splitting (DBS) was used to increase the dose efficiency by a factor of 6 compared to selected Bremsstrahlung splitting (Kawrakow and Rogers, 2003). The electron beam was modeled using source number 19 from BEAMnrc program (Rogers *et al*., 2006) and the incident electron beam was perpendicular to the target. The spatial resolution of the electron beam in 2 dimensions was defined by the Gaussian distribution with the Full Width at Half Maximum (FWHM) = 1.6 mm. The electron energy was a spectrum and the central energy was 6.8 MeV. The CPU used for the simulation was Intel® Core (TM)2 Quad CPU Q8400 with 2.67 GHz processors and 4 GB memory (RAM).

The output phase space file from BEAMnrc (z = 100 cm) was used as the input in DOSXYZnrc to calculate the dose profile and percentage depth dose in a water phantom (50×50×50 cm^3). The phantom was divided into 81×81×31 detectors in x, y and z directions. The volume of the voxels was changed from 0.008-0.04 cm^3. The dimension of the detectors was small in build up and high gradient regions to have a good spatial resolution. In the depths after d_{max} (>1.5 cm), the detector dimension in the z-axis was changed to a larger value but the dimensi.

Convolution of IMRT treatment plans: Five IMRT plans for nasopharynx cancer were selected for verification using the step-and-shoot technique with 6 MV photons. The cancer stage of IMRT1, IMRT2 and IMRT4 was T2 N2 M0 while IMRT3 was T4 N2 M0 and IMRT5 was T3 N2 M0. Each plan had 9 fields and an average of 90 segments. The IMRT plans for

nasopharynx normally have steep gradients which usually give rise to a low passing rate using 3% DD (dose difference) and 3 mm DTA (distance to agreement). Plan verification was performed on the solid water phantom which was 8 cm thick on the surface of the I'mRT MatriXX and the source to the EPOM distance was 100 cm using 6 MV as shown in Fig. 1b. For the reference measurement a 0.6 cm^3 Farmer chamber (FC65-G) was placed at depth 4 cm with 4 cm backscattering phantom slabs.

Every plan was measured with the central beam axis oriented in the center and perpendicular to the surface of the 2D array, the gantry angle being zero degree. A CT containing the phantom set-up with the 2D array was exported to calculate the dose distribution of the IMRT plans using Oncentra Master Plan treatment planning system. The dose points measured by the I'mRT MatriXX array were interpolated from 0.76-0.1 cm. The TPS dose plan was first integrated from 0.2-0.76 cm and the interpolated back to 0.1 cm for cross plan dose profile comparison using OmniPro software. The cross plan dose profiles of a 6 MV photon beam of IMRT plans using both the 2D array as well as TPS were obtained. The measured values of the 2D array were then compared with the convolved values of the calculated dose profile (TPS) using the single-detector line spread function.

RESULTS AND DISCUSSION

Applying the convolution for different field sizes: Regarding to the previous study (Alashrah *et al*., 2013), the maximum variation was less than 10% for all the field sizes when the convolution method was applied. Before the convolution, the maximum difference between the measured profiles and true profiles was more than 50% especially in the high gradient regions for the small field size of 2×2 cm^2, as shown in Fig. 3. Small field sizes are normally used in IMRT. For the larger field sizes (15×15 cm^2 and 20×20 cm^2), the maximum difference between the measured profiles and true profiles was less than 5% in the high and low gradient regions as shown in Fig. 3. The selected Gaussian function of the single chamber response in the I'mRT MatriXX was found to be a good fit for all field sizes from 2×2 cm^2 to 20×20 cm^2. Hence, the function can be used to verify IMRT plans which have fields of different sizes. This was performed for only 6 MV photons as this was the energy used in patient IMRT treatment at the hospital.

For field profiles obtained from the Monte Carlo simulation, EBT2 film and IC03, the maximum difference in the low gradient region was within 2% and in the high gradient region was less than 3.5% between the three methods for all field sizes used in this study (Fig. 4). The good agreement in the steep gradient profiles from Monte Carlo simulation and EBT2 film with the true dose profile from IC03 clearly shows that both methods permit the measure of the true dose profiles with sufficient accuracy. This is to be expected as the voxel sizes were 0.008 cm^3 in the high gradient region for Monte Carlo simulation, point size for EBT2 film and 0.028 cm^3 for IC03. However the ionization chamber in the 2D array has a volume of 0.08 cm^3. Similar results have been reported using EDR2 film, MOSFET dosimeters, IC03 and Monte Carlo calculation (Lydon, 2005).

At field sizes larger than 5×5 cm^2 the fraction of pixels passing gamma index at 3%/3 mm criteria between the calculated with convolution correction and the measured profiles was above 90%. The relative number of test points associated with the penumbra regions which are the regions causing the non-passing of the gamma index both for the

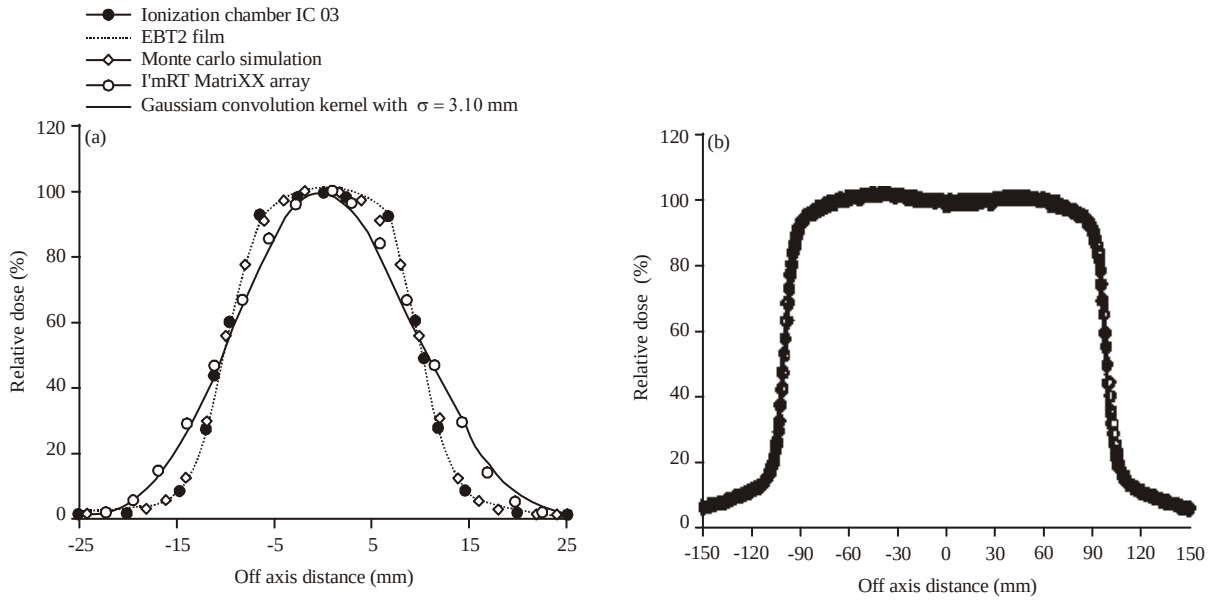

Fig. 3(a-b): Comparison between the dose profiles of various 6 MV photon fields at 5 cm phantom depth for field size (a) 2×2 cm^2 and (b) 20×20 cm^2

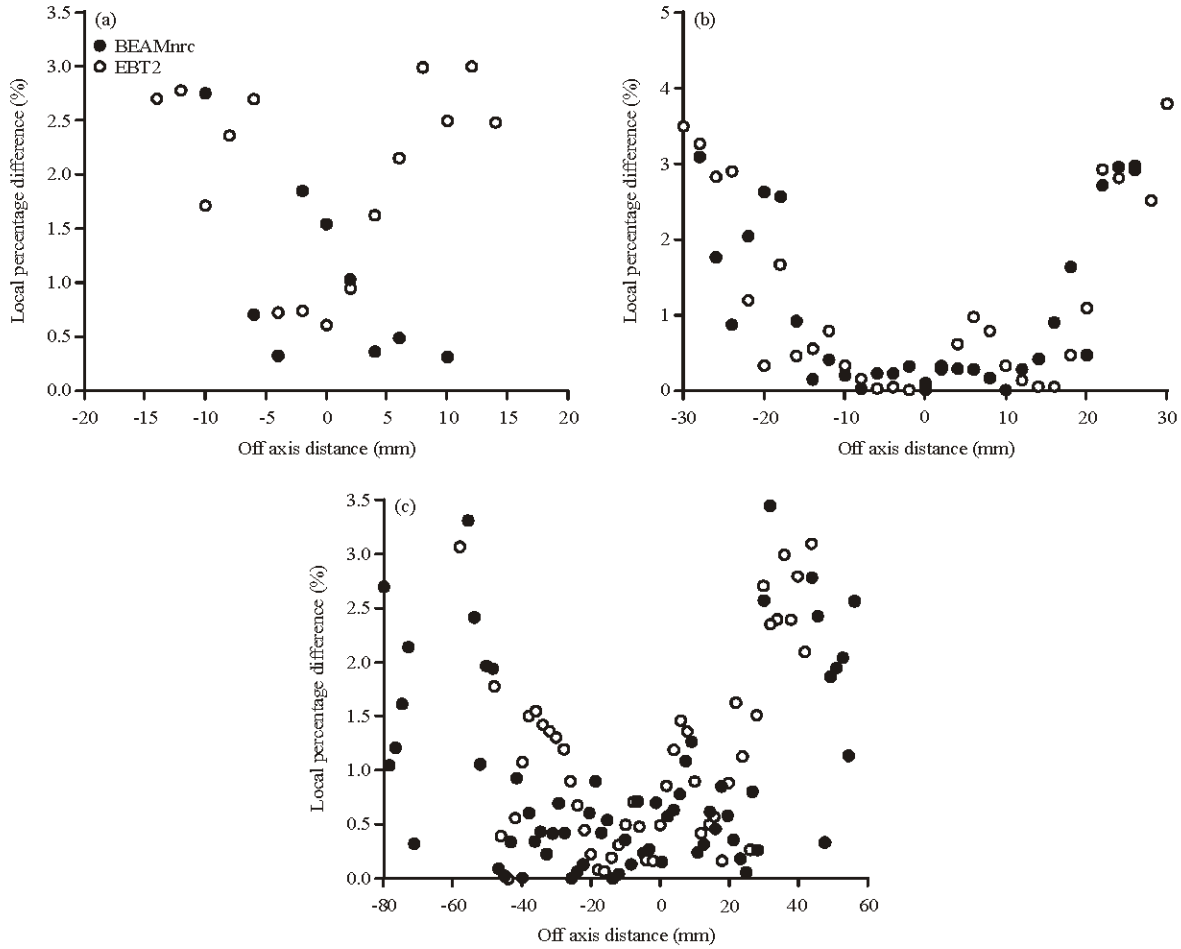

Fig. 4(a-c): Local Percentage Difference (LPD) between IC03 and either BEAMnrc or EBT2 film for field sizes (a) 2×2 cm^2, (b) 5×5 cm^2 and (c) 10×10 cm^2. The maximum difference was between 3 and 4% in the steep dose gradients

Table 1: Ratio of the points in the penumbra (20-80%) over the total field in both the non-convolved and convolved TPS. R is the right penumbra region whilst L is the left penumbra region

	Relative number of points (%)			
	Non-convolved TPS		Convolved TPS	
Field size (cm^2)	R	L	R	L
2×2	28	26	25	25
5×5	15	15	10	10
10×10	10	11	9	9

calculated with convolution correction and the measured profiles was above 90%. The relative number of test points associated with the penumbra regions which are the regions causing the non-passing of the gamma index both for the non-convolved and convolved the TPS values becomes smaller with increasing field sizes. For the 2×2 cm^2 field, the relative number of test points in the penumbra region is 26-28% which then dropped to 10-11% for the 10×10 cm^2 field in the non-convolved TPS (Table 1). Therefore, the convolution method should be applied especially for small field sizes to reduce the deviation between the calculated and the measured profiles.

Applying the convolution for NPC IMRT cases: Figure 5a-c shows the profiles in the cross-plan directions for the TPS readings before and after convolution as well as the I'mRT MatriXX measurements for three nasopharynx IMRT plans which had low gamma index. Better agreement between the measured data and the convolved TPS data was obtained. The maximum deviation between the measured profile and the corrected profile was 5% in both regions of steep and low gradients. Without the correction, the maximum deviation between the measured profile and the uncorrected TPS plan profile was within 20%. Discrepancy between calculated cross-profiles of intensity modulated beams and measured intensity modulated profiles using Kodak EDR2 film has been reported by Laub and Wong (2003) to be more than 10% where film is known to have good spatial resolution.

The OmniPro software was used to calculate the gamma index between the planar TPS (Oncentra Master Plan) plan and the measured plan using I'mRT MatriXX detector under similar conditions. The gamma index of the cross profiles of the fields were also calculated for TPS plans before and after convolution with respect to I'mRT MatriXX measured dose distribution using Excel. Presently, the OmniPro I'mRT v1.5

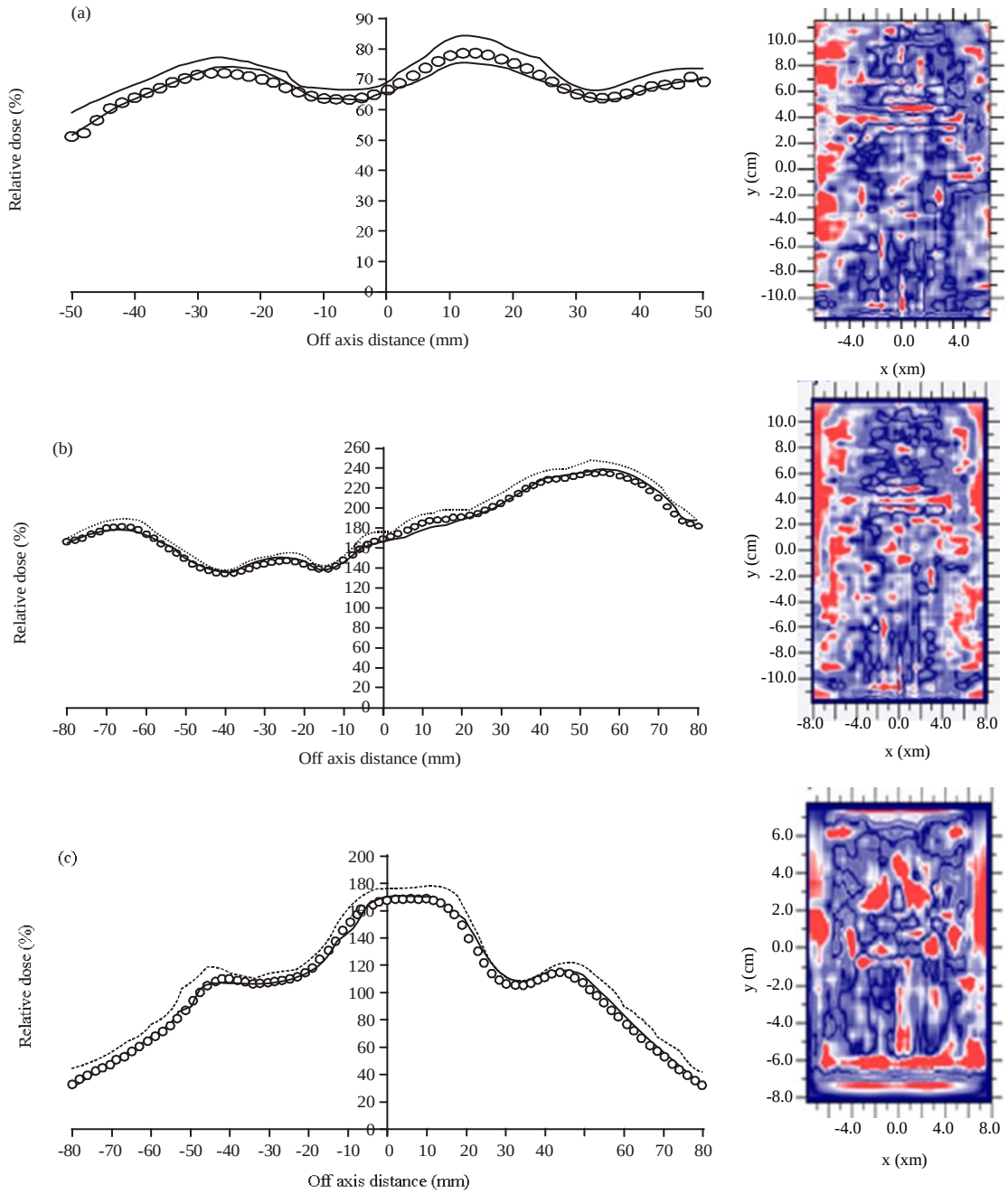

Fig. 5(a-c): Dose profile of three IMRT plans (a) IMRT3, (b) IMRT5 and (c) IMRT4 for head and neck calculated by TPS and measured by I'mRT MatriXX 6 MV, SSD 91.6 cm, 8 cm depth in RW3

software does not allow the convolution of TPS profiles (Herzen *et al*., 2007) For gamma criteria at 3%/3 mm, the passing rates obtained in these comparisons are shown in Table 1. For IMRT3 before convolution only 80.2% of pixels passed gamma criteria (3%/3 mm) but improved significantly to 90.7% when the Gaussian convolution kernel was applied as shown in Table 2.

In Table 2 the red regions in the gamma index plot have gamma index larger than 1 which indicates that the pixels in this region have failed the gamma index. Treatment plans of nasopharynx cancer have steep gradients which give rise to poor passing rates when TPS plans without convolution are compared to measurements by 2D array. The IMRT cases where less than 82% pixels pass the gamma criteria had late stage nasopharynx cancer (T4 and T3) and the tumors had spread to larger areas. These areas were close to the organs at risk and more stringent contouring was applied. The smallest segments in the IMRT plans have an area of 4 cm^2. It is

Table 2: Passing rates between I'mRT MatriXX and TPS dose distributions before and after convolution correction at gamma criteria 3%/3 mm for field sizes from 2×2 till 10×10 cm^2 and five IMRT plans

	I'mRT MatriXX with TPS (%)	
Field size (cm^2)	Before correction	After correction
2×2	43.7	89.5
5×5	86.8	96.6
8×8	88.7	95.5
10×10	92.1	98.6
IMRT1	90.4	96.7
IMRT2	94.6	100.0
IMRT3	80.2	92.7
IMRT4	82.2	94.0
IMRT5	80.3	93.6

important clinically that TPS plans with steep gradients are first convolved with the Gaussian function before being verified by I'mRT MatriXX.

CONCLUSION

Low spatial resolution in the penumbra region encountered in a 2D array I'mRT MatriXX can be improved by applying the Gaussian convolution kernel. The Gaussian convolution kernel was used to convolve the true dose profile of five nasopharynx IMRT plans obtained by Treatment Planning System (TPS). Gafchromic film (EBT2) and Monte Carlo simulation were also used to verify the true dose profiles of different field sizes. Good agreement in the dose profiles between I'mRT MatriXX, IC03, EBT2 film and the Monte Carlo simulation were observed in the low gradient region. In the steeper dose gradients better agreement between I'mRT MatriXX and IC03 was obtained after the Gaussian convolution kernel was applied to the IC03 data. The convolved dose distribution for IMRT plans were compared with the measured plans of the a 2D array I'mRT MatriXX. The passing rates improved significantly from 80.2-92.2% using the 3%/3 mm gamma index criteria when the cross dose profile plans from the treatment planning system were convolved. Convolution can minimize the difference in the beam profiles which occur in the I'mRT MatriXX detector due to the finite size of the detector and the transport of the secondary electrons into the detector.

ACKNOWLEDGMENTS

We are indebted to Universiti Sains Malaysia for providing us a short-term grant and to the Radiotherapy Unit of the Mt. Miriam Hospital in Penang, Malaysia, for the use of the LINAC and the I'mRT MatriXX. S. Alashrah was financially supported by the Qassim University.

REFERENCES

Alashrah, S., S. Kandaiya, L.S. Lum and S.K. Cheng, 2013. Depth dependence of the single chamber response function of the I'mRT MatriXX array in a 6 MV photon beam. Zeitschrift Medizinische Physik, 23: 270-278.

Alashrah, S., S. Kandaiya, N. Maalej and A. El-Taher, 2014. Skin dose measurements using radiochromic films, TLDS and ionisation chamber and comparison with Monte Carlo simulation. Radiat. Prot. Dosimetry, 162: 338-344.

Alashrah, S., S. Kandaiya, S.Y. Yong and S.K. Cheng, 2010. Characterization of a 2D ionization chamber array for IMRT plan verification. Nucl. Instrum. Methods Phys. Res. Sect. A: Acceler. Spectrom. Detect. Assoc. Equip., 619: 181-185.

Arjomandy, B., N. Sahoo, X. Ding and M. Gillin, 2008. Use of a two-dimensional ionization chamber array for proton therapy beam quality assurance. Med. Phys., 35: 3889-3894.

Arnfield, M.R., K. Otto, V.R. Aroumougame and R.D. Alkins, 2005. The use of film dosimetry of the penumbra region to improve the accuracy of intensity modulated radiotherapy. Med. Phys., 32: 12-18.

Bednarz, G., M.S. Huq and U.F. Rosenow, 2002. Deconvolution of detector size effect for output factor measurement for narrow Gamma Knife radiosurgery beams. Phys. Med. Biol., 47: 3643-3649.

Charland, P., E. El-Khatib and J. Wolters, 1998. The use of deconvolution and total least squares in recovering a radiation detector line spread function. Med. Phys., 25: 152-160.

Chetty, I.J., B. Curran, J.E. Cygler, J.J. DeMarco and G. Ezzell *et al*., 2007. Report of the AAPM Task Group No. 105: Issues associated with clinical implementation of Monte Carlo-based photon and electron external beam treatment planning. Med. Phys., 34: 4818-4853.

Chu, R.D.H., D.F. Lewis, K.P.J. O'Hara, B.W. Buckland, F. Dinelle and G. Van Dyk, 1990. Gafchromic™ dosimetry media: A new high dose, thin film routine dosimeter and dose mapping tool. Int. J. Radiat. Applic. Instrum. Part C: Radiat. Phys. Chem., 35: 767-773.

Devic, S., J. Seuntjens, G. Hegyi, E.B. Podgorsak and C.G. Soares *et al*., 2004. Dosimetric properties of improved GafChromic films for seven different digitizers. Med. Phys., 31: 2392-2401.

Fischer, M., M. Todorovic, E. Drud and F. Cremers, 2010. Commissioning of a double-focused micro multileaf collimator (μMLC). J. Applied Clin. Med. Phys., 11: 81-91.

Fox, C., T. Simon, B. Simon, J.F. Dempsey and D. Kahler *et al*., 2010. Assessment of the setup dependence of detector response functions for mega-voltage linear accelerators. Med. Phys., 37: 477-484.

Gago-Arias, A., L. Brualla-Gonzalez, D.M. Gonzalez-Castano, F. Gomez and M.S. Garcia *et al*., 2012. Evaluation of chamber response function influence on IMRT verification using 2D commercial detector arrays. Phys. Med. Biol., 57: 2005-2020.

Garcia-Vicente, F., J.M. Delgado and C. Rodriguez, 2000. Exact analytical solution of the convolution integral equation for a general profile fitting function and Gaussian detector kernel. Phys. Med. Biol., 45: 645-650.

Han, Z., S.K. Ng, M.S. Bhagwat, Y. Lyatskaya and P. Zygmanski, 2010. Evaluation of MatriXX for IMRT and VMAT dose verifications in peripheral dose regions. Med. Phys., 37: 3704-3714.

Herzen, J., M. Todorovic, F. Cremers, V. Platz, D. Albers, A. Bartels and R. Schmidt, 2007. Dosimetric evaluation of a 2D pixel ionization chamber for implementation in clinical routine. Phys. Med. Biol., 52: 1197-1208.

Kamomae, T., Y. Miyabe, A. Sawada, O. Matoba and M. Nakata *et al*., 2011. Simulation for improvement of system sensitivity of radiochromic film dosimetry with different band-pass filters and scanner light intensities. Radiol. Phys. Technol., 4: 140-147.

Kawrakow, I. and D.W.O. Rogers, 2003. The EGSnrc code system: Monte Carlo simulation of electron and photon transport. NRCC Report No. PIRS-701, November 7, 2003.http://www.tfsoft.org.ua/~blinkenlichten/books/updated_lectures/lectures_VIVR/addons/EGSnrc (EGS4)/pirs701.pdf

Laub, W.U. and T. Wong, 2003. The volume effect of detectors in the dosimetry of small fields used in IMRT. Med. Phys., 30: 341-347.

Li, J.G., G. Yan and C. Liu, 2009. Comparison of two commercial detector arrays for IMRT quality assurance. J. Applied Clin. Med. Phys., 10: 62-74.

Looe, H.K., T.S. Stelljes, S. Foschepoth, D. Harder, K. Willborn and B. Poppe, 2013. The dose response functions of ionization chambers in photon dosimetry-Gaussian or non-Gaussian? Zeitschrift Medizinische Physik, 23: 129-143.

Lydon, J.M., 2005. Theoretical and experimental validation of treatment planning for narrow MLC defined photon fields. Phys. Med. Biol., 50: 2701-2714.

Matney, J.E., B.C. Parker, D.W. Neck, G. Henkelmann and I.I. Rosen, 2010. Evaluation of a commercial flatbed document scanner and radiographic film scanner for radiochromic EBT film dosimetry. J. Applied Clin. Med. Phys., 11: 198-208.

Meeks, S.L., F.J. Bova, S. Kim, W.A. Tome, J.M. Buatti and W.A. Friedman, 1999. Dosimetric characteristics of a double-focused miniature multileaf collimator. Med. Phys., 26: 729-733.

Pappas, E., T.G. Maris, A. Papadakis, F. Zacharopoulou, J. Damilakis, N. Papanikolaou and N. Gourtsoyiannis, 2006. Experimental determination of the effect of detector size on profile measurements in narrow photon beams. Med. Phys., 33: 3700-3710.

Paskalev, K.A., J.P. Seuntjens and E.B. Podgorsak, 2002. Dosimetry of Ultra Small Photon Fields. In: Recent Developments in Accurate Radiation Dosimetry, Seuntjens, J.P. and P.N. Mobit (Eds.). Medical Physics Publishing, Madison, WI., USA., pp: 298-318.

Poppe, B., A. Blechschmidt, A. Djouguela, R. Kollhoff, A. Rubach, K.C. Willborn and D. Harder, 2006. Two-dimensional ionization chamber arrays for IMRT plan verification. Med. Phys., 33: 1005-1015.

Poppe, B., A. Djouguela, A. Blechschmidt, K. Willborn, A. Ruhmann and D. Harder, 2007. Spatial resolution of 2D ionization chamber arrays for IMRT dose verification: Single-detector size and sampling step width. Phys. Med. Biol., 52: 2921-2935.

Richley, L., A.C. John, H. Coomber and S. Fletcher, 2010. Evaluation and optimization of the new EBT2 radiochromic film dosimetry system for patient dose verification in radiotherapy. Phys. Med. Biol., 55: 2601-2617.

Rogers, D.W.O., B. Walters and I. Kawrakow, 2006. BEAMnrc users manual. NRCC Report No. PIRS-0509, National Research Council of Canada, Ottawa, Canada.

Rogers, D.W.O., B.A. Faddegon, G.X. Ding, C.M. Ma, J. We and T.R. Mackie, 1995. BEAM: A Monte Carlo code to simulate radiotherapy treatment units. Med. Phys., 22: 503-524.

Spezi, E., A.L. Angelini, F. Romani and A. Ferri, 2005. Characterization of a 2D ion chamber array for the verification of radiotherapy treatments. Phys. Med. Biol., 50: 3361-3373.

Tacke, M.B., S. Nill, P. Haring and U. Oelfke, 2008. 6 MV dosimetric characterization of the 160 MLC™, the new Siemens multileaf collimator. Med. Phys., 35: 1634-1642.

Ulmer, W. and W. Kaissl, 2003. The inverse problem of a Gaussian convolution and its application to the finite size of the measurement chambers/detectors in photon and proton dosimetry. Phys. Med. Biol., 48: 707-727.

Van't Veld, A.A., P. Van Luijk, F. Praamstra and P.C. Van Der Hulst, 2001. Detector line spread functions determined analytically by transport of Compton recoil electrons. Med. Phys., 28: 738-751.

Vandana, S., V.S. Shaiju, S.D. Sharma, S. Mhatre, S. Shinde, G. Chourasiya and Y.S. Mayya, 2011. Dosimetry of gamma chamber blood irradiator using Gafchromic EBT film. Applied Radiat. Isotopes, 69: 130-135.

Yan, G., C. Fox, C. Liu and J.G. Li, 2008. The extraction of true profiles for TPS commissioning and its impact on IMRT patient-specific QA. Med. Phys., 35: 3661-3670.

Zeidan, O.A., S.A.L. Stephenson, S.L. Meeks, T.H. Wagner, T.R. Willoughby, P.A. Kupelian and K.M. Langen, 2006. Characterization and use of EBT radiochromic film for IMRT dose verification. Med. Phys., 33: 4064-4072.